Heliyon 10 (2024) e23867

Contents lists available at ScienceDirect

Heliyon

journal homepage: www.cell.com/heliyon

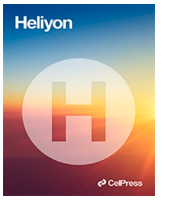

The role of serum acylcarnitine profiling for the detection of multiple solid tumors in humans

Longjunyu Wu [1], Chunhua Ye [1], Qingchun Yao [1], Qianqian Li, Chunyan Zhang [**], Yuandong Li [*]

Department of Research, Guangxi Medical University Cancer Hospital, Nanning, 530021, Guangxi Zhuang Autonomous Region, China

ARTICLE INFO

Keywords:
Solid tumors
Fatty acid oxidation
Acylcarnitines
Metabolic reprogramming
Metabolomics

ABSTRACT

Metabolic reprogramming is an essential hallmark of cancer. Several studies have reported the dysregulation of acylcarnitine (ACar) metabolism in tumor cells, suggesting that changes in the blood ACar may be related to tumor growth. Accordingly, this study aimed to understand the alteration of serum ACar profiles in various solid tumors and explore the potential of differential serum ACars as diagnostic biomarkers. A series of 69 relatively abundant ACars were identified via untargeted analysis. Then, targeted metabolomics was used to describe the metabolic alterations in ACars between normal controls and patients with six types of solid tumors. The results suggested that changes in ACars correlated with their carbon chain length and saturation. The six tumor types had highly similar ACar metabolic profiles, indicating similar fatty acid oxidation (FAO) metabolic pathways. Moreover, the receiver operating curve analysis of differential ACars showed that 16 ACars (C8–C14) had high diagnostic capability towards the studied solid tumors. Specifically, the area under the curve of ACar 10:2 isomer2 and ACar 12:2 isomer2 was greater than 0.95. In conclusion, the marked decrease in the levels of medium- and long-chain ACars (C8–C18) in the six solid tumors suggests that they may have similar FAO-based metabolic pathways, which could afford a common target for cancer therapy. Additionally, 16 ACars (C8–C14) were identified as potential biomarkers for diagnosing six types of solid tumors.

1. Introduction

Cancer is one of the leading causes of death globally [1]. Accurate early diagnosis of cancers is critical in the management of the disease. Although several techniques are widely used for cancer screening, most of these are invasive. Recently, several non-invasive methods have been studied extensively for diagnosing cancer. Specifically, non-invasive diagnosis via blood analysis is a promising advancement in cancer research [2–5]. Solid tumors, such as hepatocellular carcinoma (HCC), gastric cancer (GC), colorectal cancer (CRC), lung cancer (LCA), primary liver cancer without HCC (e.g., intrahepatic cholangiocarcinoma and mixed liver cancer) (PLC-NHCC), are usually detected in advanced stages. As a result, many cases of solid tumors are often diagnosed when the cancers

* Corresponding author. Department of Research, Guangxi Medical University Cancer Hospital, 71 Hedi Road, Nanning, 530021, Guangxi Zhuang Autonomous Region, China.
** Corresponding author. Department of Research, Guangxi Medical University Cancer Hospital, 71 Hedi Road, Nanning, 530021, Guangxi Zhuang Autonomous Region, China.
E-mail addresses: zcy_263@163.com (C. Zhang), lyd641209@163.com (Y. Li).
[1] These authors contributed equally to this work.

https://doi.org/10.1016/j.heliyon.2023.e23867
Received 28 March 2023; Received in revised form 28 November 2023; Accepted 14 December 2023
Available online 19 December 2023

Abbreviations

ACar	acylcarnitine
AUC	area under the curve
CE	collision energy
COT	carnitine octanoyltransferase
CPT	carnitine palmitoyltransferase
CRC	colorectal cancer
DP	declustering potential
ESI	electrospray ionization
FAO	fatty acid oxidation
FC	fold change
GC	gastric cancer
HBV-HCC	hepatitis B virus-related hepatocellular carcinoma
HCC	hepatocellular carcinoma
Hif	hypoxia-inducible factors
HR MRM	high-resolution multiple reaction monitoring
IDA	information-dependent acquisition
LCA	lung cancer
NC	normal control
PLC-NHCC	primary liver cancer without hepatocellular carcinoma (including intrahepatic cholangiocarcinoma and mixed liver cancer)
QC	quality control
QTOF-MS/MS	quadrupole time-of-flight mass spectrometry
ROC	receiver operating characteristic
RT	retention time
TME	tumor microenvironment
UHPLC-MS/MS	ultra-high performance liquid chromatography-tandem mass spectrometry

have become locally aggressive or metastasized, for which there are no effective therapies. In clinical practice, solid tumors are often screened and diagnosed using several types of serum biomarkers, such as carbohydrate antigen 19-9, alpha-fetoprotein, and carcinoembryonic antigen. However, the sensitivity and specificity of serum biomarkers are limited. Therefore, it is crucial to identify novel biomarkers for screening solid tumors.

It is well known that metabolic alterations promote carcinogenesis and the adaptation of cancer cells to the local microenvironment, a process called metabolic reprogramming [6]. Reportedly, increased aerobic glycolysis, also known as the Warburg effect, is one of the most common metabolic alterations that mediate cancer progression [7]. Such metabolic reprogramming is induced by several factors, including oncogenes, growth factors, acidosis, hypoxia-inducible factors (Hif), and dysregulation of tumor suppressor genes [8]. Under normoxia, cells preferentially utilize glucose carbon to synthesize palmitate. In contrast, under hypoxic conditions, the fatty acids are primarily synthesized from glutamine carbon via the reductive pathway [9]. This unique distribution of nutrients was intrinsically mediated by mTORC1 signaling and the expression of genes related to glucose and glutamine [10]. To date, most studies on cancer have focused on glycolysis, glutaminolysis, and fatty acid synthesis. However, the role of fatty acid oxidation (FAO) in cancer cell function has not been elucidated. Under limited glucose and glutamine availability, fatty acids are catabolized via mitochondrial β-oxidation as an alternative to ATP production [11]. The metabolic reprogramming of tumor cells is not only related to their characteristics, but also to the tumor microenvironment (TME). Research suggests that FAO is activated by specific oncogenes [12,13]. However, emerging research highlights the important role of TME. FAO can occur in both mitochondria and peroxisomes. Hypoxia and acidosis are common features of solid tumors. Hypoxic cells sense oxygen levels to modulate anabolic and catabolic pathways in response to changes in oxygen availability [14]. Studies have demonstrated that during hypoxia, Hif-2α promote the degradation of peroxisomes through selective autophagy [15]. Moreover, the metabolic properties of tumors directly lead to the acidification of the TME. Acidosis alters the metabolic processes of cancer cells toward FAO [16]. Therefore, it is also increasingly evident that FAO plays a critical role in the initiation and progression of various cancers [17]. A recent study has suggested that tumors originating in different tissues and those of different histological subtypes exhibit a common proteomic signature related to energy metabolism [18]. However, different tumors demonstrate distinct and heterogeneous metabolic processes, which renders targeting metabolism in various tumor types challenging [19]. At present, no uniform, tumor-specific, metabolic signatures have been determined for solid tumors. Therefore, we hypothesized that solid tumors may share the similar FAO metabolic pathways. Understanding the characteristics of FAO pathways in solid tumors may contribute to the identification of novel diagnostic biomarkers and therapeutic targets.

ACars are esters of L-carnitine and fatty acids [20] that can transport activated, long-chain fatty acids from the cytoplasm to mitochondria for β-oxidation to provide energy for cellular activities [21]. ACar is not only an intermediate in FAO, but changes in its composition and concentration indirectly correlate with alterations in cellular metabolism. Recently, a study reported that in cancer

cells, the levels of ACars with different chain lengths were regulated by metabolic reprogramming [22], and this finding has gained considerable attention in recent years. Currently, a variety of differential ACars have been observed in a number of malignancies, including HCC [23–25], LCA [26,27], CRC [28,29], and GC [30]. However, no study has comprehensively analyzed the ACars profiles in different solid tumors. Thus, such metabolic profiling of serum ACars with different chain lengths and degrees of saturation will help assist in identifying potential diagnostic markers and therapeutic targets for various solid tumors.

Currently, ACars are commonly analyzed using ultra-high performance liquid chromatography-tandem mass spectrometry (UHPLC-MS/MS), owing to its ultra-efficient separation ability and extreme sensitivity that facilitate the simultaneous separation of isomers in a short time [31]. For the large-scale identification of most Acars, a liquid chromatography high-resolution mass spectrometry method has been developed [32]. Therefore, this method can be employed to identify ACars that are relatively abundant in the serum of quality control (QC) samples and then employ targeted metabolomics to screen for differential ACars and assess their diagnostic value in various solid tumors.

Accordingly, this study primarily aimed to understand the alteration of serum ACar profiles between normal controls (NCs) and common solid tumors using UHPLC-quadrupole time-of-flight mass spectrometry (QTOF-MS/MS) via untargeted analysis and targeted metabolomics. The solid tumors assessed were hepatitis B virus (HBV)-related HCC, GC, CRC, LCA, and PLC-NHCC. First, untargeted analysis was used to identify ACars that were relatively abundant in QC samples. Subsequently, the relative content of the identified ACars in NC, HBV-HCC, GC, CRC, LCA, and PLC-NHCC samples was determined by targeted analysis. Finally, the potential clinical diagnostic value of ACars was explored.

2. Materials and methods

2.1. Chemicals and reagents

HPLC-grade acetonitrile and formic acid were purchased from Merck (Darmstadt, Germany), and 3-hydroxydecanoyl carnitine was obtained from Sigma (Saint Louis, USA). Ultra-pure water was synthesized in the laboratory. ACQUITY BEH C18 Column (2.1 mm × 100 mm, 1.7 μm) was purchased from Waters Corporation (Milford, MA, USA). Amicon Ultra-0.5-mL Centrifugal Filter (Ultracel-3k Da) was obtained from Merck Millipore (Massachusetts, USA).

2.2. Patients and serum sample collection

In total, 172 participants visiting the Guangxi Medical University Cancer Hospital from April 2018 to September 2019 were enrolled in the study. Of these, 30 were NCs and 142 were patients with six types of cancer (41 with HBV-HCC, 23 with GC, 37 with CRC, 26 with LCA, and 15 with PLC-NHCC [including 10 with intrahepatic cholangiocarcinoma and 5 with mixed liver cancer]). All NC subjects had normal liver biochemistry, and those with liver-related diseases were excluded. The diagnosis of all patients with cancer was confirmed by histopathological biopsies. All patients with HBV-HCC were diagnosed with chronic hepatitis B cirrhosis.

Serum samples were collected from the participants in the morning after overnight fasting to eliminate the impact of diet. The samples were then left at room temperature for 30 min, followed by centrifugation at 4427×*g* for 10 min (4 °C). The supernatant was then collected and stored at −80 °C until further analysis.

The study protocol was approved by the Medical Ethics Committee of the Guangxi Medical University Cancer Hospital (ethical approval number: LW2022127), and all subjects provided written informed consent allowing the use of their samples for biomedical research.

2.3. Serum samples treatment

The frozen serum samples were thawed at room temperature for 30 min. Then, protein precipitation was performed by transferring 150 μL of serum to a 1.5-mL centrifuge tube, to which 150 μL of acetonitrile was added, vortexed for 30 s, and frozen at −20 °C for 1 h. The samples were then centrifuged at 16,602×*g* for 15 min at 4 °C. The supernatant obtained was transferred to an Amicon Ultra-0.5 mL Centrifugal Filter (Ultracel-3k Da) and centrifuged at 16,602×*g* for 15 min at 4 °C. The filtrate obtained was transferred to an injection vial. The QC sample was prepared by mixing 10 μL from each serum sample. One QC sample was run after every 15 sample injections to monitor the stability and precision of the instrument during the analysis.

2.4. UHPLC-MS/MS analysis

For UHPLC-MS/MS analysis, the ExionLC™ AC UHPLC system was coupled with a quadrupole time-of-flight tandem mass spectrometry (X500R QTOF) (AB SCIEX, USA). Initially, untargeted analysis of the QC sample was performed under the information-dependent acquisition (IDA) mode, followed by identifying ACars, as reported previously [32]. Subsequently, UHPLC-MS/MS was performed under a high-resolution multiple reaction monitoring (HR MRM) mode to analyze serum samples from NCs and patients with six types of solid tumors.

2.4.1. Liquid chromatography conditions

For UHPLC, a 5-μL sample was injected into the Waters ACQUITY BEH C18 column, maintained at 40 °C. The injection temperature was set at 4 °C, with the flow rate being 0.4 mL/min and the total run time being 23 min. Separation was achieved using a mobile phase

comprising 0.1 % formic acid in water (A) and 0.1 % formic acid in acetonitrile (B). The linear gradient elution condition was as follows: 0–9 min, 2 %→45 % B; 9–15 min, 45 %→100 % B; 15–18 min, 100 % B; 18–20 min, 100 %→2 % B; 20–23 min, 2 % B.

2.4.2. MS conditions

The mass spectrometry was operated in positive electrospray ionization (ESI) mode, with the pressure of the ion source gas 1, ion source gas 2, curtain gas, and collision activation dissociation gas being 50, 50, 35, and 8 psi, respectively. The capillary temperature and spray voltage were set at 500 °C and 5500 V, respectively. The total scan time was 23 min.

The MS parameters were as follows: *m/z* scan range of 100–1250; accumulation time of 0.10 s; declustering potential (DP), DP spread, collision energy (CE), and CE spread of 80, 0, 10, and 0 V, respectively. Under the IDA mode, we included small molecules, and the maximum candidate ions were 10. The intensity threshold was >10 cps, and dynamic background subtraction was ensured.

The parameter settings for MS/MS of untargeted analyzes were as follows: *m/z* scan range of 50–1250; DP, DP spread, CE, and CE spread of 80, 0, 35, and 15 V, respectively; and accumulation time of 0.05 s. The detailed parameters used for MS and MS/MS of targeted analyzes are listed in Supplementary Table S1.

2.5. Establishment of standard curve

Briefly, the 3-hydroxydecanoyl carnitine standard was accurately weighed at 10 mg and was dissolved and diluted in acetonitrile/water (1:1, v/v) to obtain a 3-hydroxydecanoyl carnitine standard stock solution of 2×10^9 ng/L. This stock solution was stored at 4 °C until further use. A series of standard solutions was prepared by diluting the aforementioned stock solution with acetonitrile/water (1:1, v/v). The concentrations of standard solutions prepared were 2×10^1, 1×10^2, 5×10^2, 1×10^4, 5×10^4, 2×10^5, and 1×10^6 ng/L. Under the HR MRM mode, the diluted standard solutions were sequentially injected and analyzed. Subsequently, the standard curve for 3-hydroxydecanoyl carnitine was plotted for the relative quantitative analysis of other ACars according to the peak area (Y) and concentration (X) of the characteristic product ion ($m/z = 85.0284$).

Table 1
Acylcarnitines identified in the QC sample.

No.	Metabolite	Isomer	Precursor ion (Da)	RT (min)	No.	Metabolite	Isomer	Precursor ion (Da)	RT (min)
1	L-carnitine		162.1120	0.67	36	ACar 14:1	isomer2	370.2951	11.62
2	ACar 2:0		204.1227	0.76	37	ACar 16:1		398.3265	12.12
3	ACar 3:0		218.1388	1.61	38	ACar 18:1		426.3566	12.84
4	ACar 4:0	isomer1	232.1544	2.53	39	ACar 20:1		454.3892	13.46
5		isomer2		2.64	40	ACar 10:2	isomer1	312.2170	7.74
6	ACar 5:0	isomer1	246.1702	3.57	41		isomer2		7.94
7		isomer2		3.70	42	ACar 12:2	isomer1	340.2486	9.67
8	ACar 6:0		260.1858	5.21	43		isomer2		9.82
9	ACar 8:0		288.2167	7.47	44	ACar 14:2	isomer1	368.2797	10.78
10	ACar 9:0	isomer1	302.2327	7.87	45		isomer2		10.99
11		isomer2		8.04	46		isomer3		11.25
12		isomer3		8.47	47	ACar 16:2		396.3109	11.61
13	ACar 10:0		316.2481	9.39	48	ACar 20:2		452.3737	13.01
14	ACar 11:0	isomer1	330.2639	9.86	49	ACar 10:3	isomer1	310.2016	6.98
15		isomer2		10.25	50		isomer2		7.41
16	ACar 12:0		344.2796	10.87	51	ACar 14:3		366.2640	10.14
17	ACar 13:0		358.2951	11.22	52	ACar 16:3		394.2953	11.31
18	ACar 14:0		372.3110	11.87	53	ACar 20:3		450.3581	12.61
19	ACar 16:0		400.3422	12.69	54	ACar 20:4		448.3423	12.32
20	ACar 18:0		428.3734	13.38	55	ACar 5-OH		262.1654	1.78
21	ACar 8:1	isomer1	286.2013	6.40	56	ACar 10-OH	isomer1	332.2433	7.51
22		isomer2		6.55	57		isomer2		7.62
23		isomer3		6.94	58	ACar 12-OH	isomer1	360.2747	9.34
24	ACar 9:1	isomer1	300.2168	7.08	59		isomer2		9.44
25		isomer2		7.52	60	ACar 14-OH		388.3059	10.89
26	ACar 10:1	isomer1	314.2324	8.02	61	ACar 16-OH		416.3369	11.84
27		isomer2		8.39	62	ACar 14:1-OH	isomer1	386.2903	10.10
28		isomer3		8.60	63		isomer2		10.32
29		isomer4		8.92	64	ACar 18:1-OH		442.3527	12.09
30	ACar 11:1		328.2484	9.28	65	ACar 14:2-OH		384.2747	9.53
31	ACar 12:1	isomer1	342.2641	10.20	66	ACar 16:2-OH		412.3062	10.73
32		isomer2		10.42	67	ACar 8:DC		318.1914	3.81
33		isomer3		10.57	68	ACar 16:DC		430.3169	9.83
34	ACar 13:1		356.2797	10.80	69	ACar 18:1:DC		456.3321	10.46
35	ACar 14:1	isomer1	370.2951	11.35					

QC: Quality control; RT: Retention time; ACar: Acylcarnitine.

2.6. Statistical analyses

All data were analyzed using the SPSS software 25.0 (IBM Corporation, USA). The Kruskal–Wallis test with Bonferroni correction was used to compare differences in serum ACar levels between NC and different cancer groups. Results with $P < 0.05$ were considered statistically significant. For the receiver operating characteristic curve (ROC) analysis of ACar levels between NC and different cancer groups, an area under the curve (AUC) of >0.90 indicated high diagnostic significance. The point at the maximum value of the Youden index was determined as the optimal cut-off point, and the sensitivity and specificity of the Youden index for differentiating two groups were used to determine the diagnostic performance of the differential ACars.

3. Results

3.1. Study population characteristics

The study enrolled 172 participants, including 30 NCs, 41 patients with HBV-HCC, 23 patients with GC, 37 patients with CRC, 26 patients with LCA, and 15 patients with PLC-NHCC (including 10 patients with intrahepatic cholangiocarcinoma and 5 with mixed liver cancer). The relative ACar levels in NC and different cancer groups were determined using a targeted quantitative analysis. The demographic and clinical information of all subjects is presented in Supplementary Table S2.

3.2. Instrument stability and precision

The peak retention time (RT) and peak area of QC samples in total ion chromatograms overlapped well (Supplementary Fig. S1). The ions in the QC sample were selected at certain time intervals, and the changes in their mass accuracy, RT, and peak area were calculated. The deviation in mass accuracy was <5 ppm, the shift in RT was <0.1 min, and the coefficient of variation of peak area was <25 % (Supplementary Table S3). These findings confirmed the precision, stability, and repeatability of the UHPLC-MS/MS method, and the acquired data met the requirements of subsequent analysis.

3.3. Untargeted analysis of QC sample

We identified 69 ACars, including isomers, using UHPLC-QTOF-MS/MS in an untargeted analysis of the QC sample by comparing the accurate precursor ions, RT, and characteristic product ion of *m/z* 85.0284. The isomers of ACars were effectively separated using the established chromatographic method (Supplementary Figs. S2A and B). There were L-carnitine and 7 short-chain (C2–C5), 33 medium-chain (C6–C12), and 28 long-chain (C13–C20) ACars (Table 1).

3.4. Standard curve of 3-hydroxydecanoyl carnitine

The standard curve of 3-hydroxydecanoyl carnitine was determined to be as follows: $Y = 1.21540\ X$ ($r^2 = 0.99994$, $n = 7$). For serum samples, the curve was linear over the concentration range of 2×10^1 ng/L ~1×10^6 ng/L (Supplementary Fig. S3). The limit of detection, where the signal-to-noise ratio equaled 3, was 3×10^1 ng/L. The limit of quantification, where the signal-to-noise ratio equaled 10, was 1×10^2 ng/L.

3.5. Relative ACar quantitation and assessment of potential ACar diagnostic markers

The HR MRM method with UHPLC-MS/MS was used for the relative quantification of the 69 ACars identified in the serum (Supplementary Table S1). Except for ACar 2:0, all other ACars could be quantified using a standard curve established for 3-hydroxydecanoyl carnitine. For ACar 2:0, relative quantification could not be performed owing to its overload.

3.5.1. Metabolic differences in ACars between NC and HBV-HCC samples

A total of 47 serum ACars were significantly different between NC and HBV-HCC groups ($P < 0.05$; 44 ACars, $P < 0.01$; 37 ACars, $P < 0.001$). The fold changes (FCs) of 37 of these ACars (C8–C16, $P < 0.001$) ranged from 2.02 to 4.26. Except for the level of ACar 8:DC, the levels of the remaining 46 ACars decreased in the HBV-HCC group (Table 2, Supplementary Table S4). Further ROC analysis showed that 30 ACars had AUC >0.90 for diagnosing HBV-HCC, with 14 ACars (C8–C13) having AUC >0.95 (Table 3, Supplementary

Table 2
The number of acylcarnitines significantly altered in the studied solid tumors.

	$P < 0.05$	$P < 0.01$	$P < 0.001$
NC vs HBV-HCC	47	44	37
NC vs GC	57	52	48
NC vs CRC	56	54	49
NC vs LCA	58	54	49
NC vs PLC-NHCC	50	45	35

Table S4).

3.5.2. Differences in ACar metabolism between NC and GC groups

In total, 57 serum ACars differed significantly between NC and GC groups ($P < 0.05$; 52 ACars, $P < 0.01$; 48 ACars, $P < 0.001$). The FC of 48 ACars (C8–C18, $P < 0.001$) ranged from 2.01 to 7.74. Except for the levels of ACar 5-OH and ACar 8:DC, the levels of remaining ACars decreased in the GC group (Table 2, Supplementary Table S5). Furthermore, ROC analysis revealed that 40 ACars had an AUC of >0.90 for diagnosing GC, with 28 ACars (C8–C14) having an AUC of >0.95 (Table 3, Supplementary Table S5).

3.5.3. Differences in ACar metabolism between NC and CRC

In total, 56 ACars differed significantly between NC and CRC groups ($P < 0.05$; 54 ACars, $P < 0.01$; 49 ACars, $P < 0.001$). The FC of 49 ACars (C8–C18, $P < 0.001$) ranged from 1.88 to 5.44. Except for the level of ACar 8:DC, the levels of the remaining 55 ACars decreased in the CRC group (Table 2, Supplementary Table S6). In addition, 19 ACars had an AUC of >0.90 for diagnosing CRC, with 3 ACars (C10–C12) having AUC >0.95 (Table 3, Supplementary Table S6).

3.5.4. Differences in ACar metabolism between NC and LCA groups

Overall, 58 serum ACars differed significantly between NC and LCA groups ($P < 0.05$; 54 ACars, $P < 0.01$; 49 ACars, $P < 0.001$). The FC of 49 ACars (C8–C18, $P < 0.001$) ranged from 2.79 to 7.20. The level of ACars was lower in the LCA group than in the NC group (Table 2, Supplementary Table S7). In addition, 40 ACars had an AUC of >0.90 for diagnosing LCA, with 29 ACars (C8–C16) having an AUC of >0.95 (Table 3, Supplementary Table S7).

3.5.5. Differences in ACar metabolism between NC and PLC-NHCC groups

In total, 50 ACars differed significantly between NC and PLC-NHCC groups ($P < 0.05$; 45 ACars, $P < 0.01$; 35 ACars, $P < 0.001$). The FC of 35 ACars (C8–C16, $P < 0.001$) ranged from 2.48 to 5.86. Except for the level of ACar 8:DC, the levels of the remaining ACars were lower in the PLC-NHCC group than in the NC group (Table 2, Supplementary Table S8). In addition, 32 ACars had an AUC of >0.90 for diagnosing PLC-NHCC, with 19 ACars (C8–C14) having an AUC of >0.95 (Table 3, Supplementary Table S8).

3.5.6. Differences in ACar metabolism between NC and all the studied cancers

A total of 43 ACars (C8–C18) differed significantly between NC and HBV-HCC, GC, CRC, LCA, and PLC-NHCC (intrahepatic cholangiocarcinoma and mixed liver cancer) groups (all $P < 0.05$) (Fig. 1), with 31 ACars (C8–C16) differing with a P-value of <0.001 (Table 4). Fig. 2 shows an overview of the FC observed in ACar profiles when comparing the solid tumors with NCs. The six types of solid tumors may share the similar fatty acid energy metabolic profiles. In addition, the levels of medium- and long-chain, saturated ACars were significantly lower in solid tumors than in NCs (Fig. 3A–E). This suggests a possible correlation between changes in ACars and their chain length and saturation.

ROC analysis demonstrated that 16 ACars (C8–C14) had AUC values of >0.90 for the diagnosis of all six solid tumors, with ACar 10:2 isomer2 and 12:2 isomer2 having an AUC of >0.95 (Table 5). The relative concentrations of ACar 10:2 isomer2 and 12:2 isomer2 in the solid tumors were lower than those in NCs (Fig. 4A and B). Furthermore, ACar 10:2 isomer2 and 12:2 isomer2 had a high AUC, along with high sensitivity and specificity for the diagnosis of the six tumor types (Fig. 5A and B).

4. Discussion

This study primarily aimed to better understand the ACar profiles with different chain lengths and degrees of saturation in six solid tumor types. As metabolic intermediates of FAO, ACars play an important role in the transport of fatty acids from the mitochondrial outer membrane to the mitochondrial matrix to provide energy for cells [33]. Moreover, ACars are increasingly being recognized as crucial biomolecules in metabolomics research and being identified as potential diagnostic biomarkers of many diseases [34]. Therefore, monitoring changes in ACar levels in solid tumors from a metabolomic perspective will facilitate the identification of new diagnostic biomarkers and treatment targets.

In the present study, 69 ACars were evaluated, including short-chain, medium-chain, long-chain, hydroxyl, branched, unsaturated, and dicarboxylic ACars. The mass spectrometric data of these ACars suggested that the specific types of ACars differed significantly between solid tumors and NCs. Specifically, 43 ACars (C8–C18) differed significantly across the six solid tumor types (Fig. 1). The

Table 3
The number of acylcarnitines with an AUC of >0.90 for the diagnosis of different solid tumors.

	AUC>0.90	AUC>0.95
NC vs HBV-HCC	30	14
NC vs GC	40	28
NC vs CRC	19	3
NC vs LCA	40	29
NC vs PLC-NHCC	32	19
NC vs All cancers	16	2

AUC: Area under the curve.

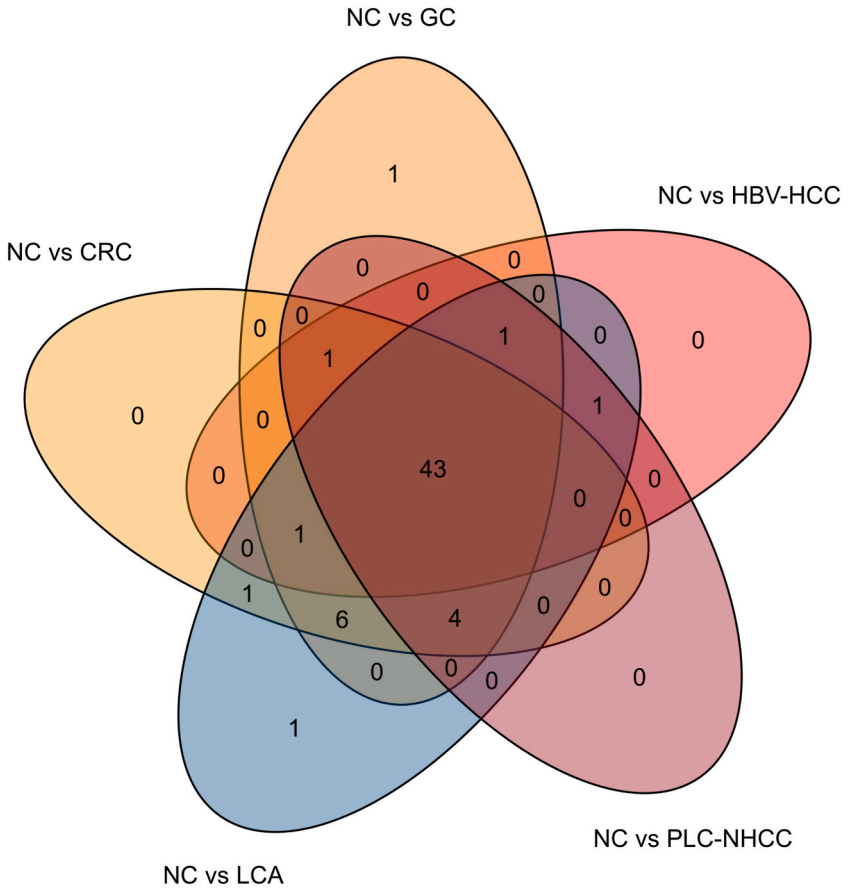

Fig. 1. Acylcarnitines significantly altered in the studied solid tumors. The Venn diagram showed the overlap of the significantly altered ($P < 0.05$) acylcarnitines among different solid tumor groups.

Table 4
Thirty-one acylcarnitines were significantly altered (all $P < 0.001$) in the studied solid tumors.

No.	Metabolite	Isomer	(M + H)+	RT (min)	No.	Metabolite	Isomer	(M + H)+	RT (min)
1	Acar 8:0		288.2167	7.47	17	Acar 10:2	isomer1	312.2170	7.74
2	Acar 9:0	isomer1	302.2327	7.87	18	Acar 10:2	isomer2	312.2170	7.94
3	Acar 9:0	isomer2	302.2327	8.04	19	Acar 12:2	isomer1	340.2486	9.67
4	Acar 9:0	isomer3	302.2327	8.47	20	Acar 12:2	isomer2	340.2486	9.82
5	Acar 10:0		316.2481	9.39	21	Acar 14:2	isomer1	368.2797	10.78
6	Acar 11:0	isomer1	330.2639	9.86	22	Acar 14:2	isomer2	368.2797	10.99
7	Acar 11:0	isomer2	330.2639	10.25	23	Acar 16:2		396.3109	11.61
8	Acar 12:0		344.2796	10.87	24	Acar 14:3		366.2640	10.14
9	Acar 8:1	isomer3	286.2013	6.94	25	Acar 10-OH	isomer1	332.2433	7.51
10	Acar 9:1	isomer2	300.2168	7.52	26	Acar 10-OH	isomer2	332.2433	7.62
11	Acar 10:1	isomer3	314.2324	8.60	27	Acar 12-OH	isomer1	360.2747	9.34
12	Acar 10:1	isomer4	314.2324	8.92	28	Acar 12-OH	isomer2	360.2747	9.44
13	Acar 12:1	isomer2	342.2641	10.42	29	Acar 14-OH		388.3059	10.89
14	Acar 12:1	isomer3	342.2641	10.57	30	Acar 14:1-OH	isomer1	386.2903	10.10
15	Acar 13:1		356.2797	10.80	31	Acar 14:2-OH		384.2747	9.53
16	Acar 14:1	isomer2	370.2951	11.62					

RT: Retention time.; ACar: Acylcarnitine.

findings suggested that solid tumors selectively consume specific ACars from the circulating blood. Reportedly, the metabolic fate of fatty acids depends on their chain length and the degree of saturation [35]. In line with this, our study demonstrated that the metabolic changes in ACars were associated with their chain length and degree of saturation (Fig. 3, Table 4). The results additionally suggest that the six solid tumors had highly similar ACar metabolic profiles, indicating metabolism via similar FAO pathways (Figs. 1, Fig. 2).

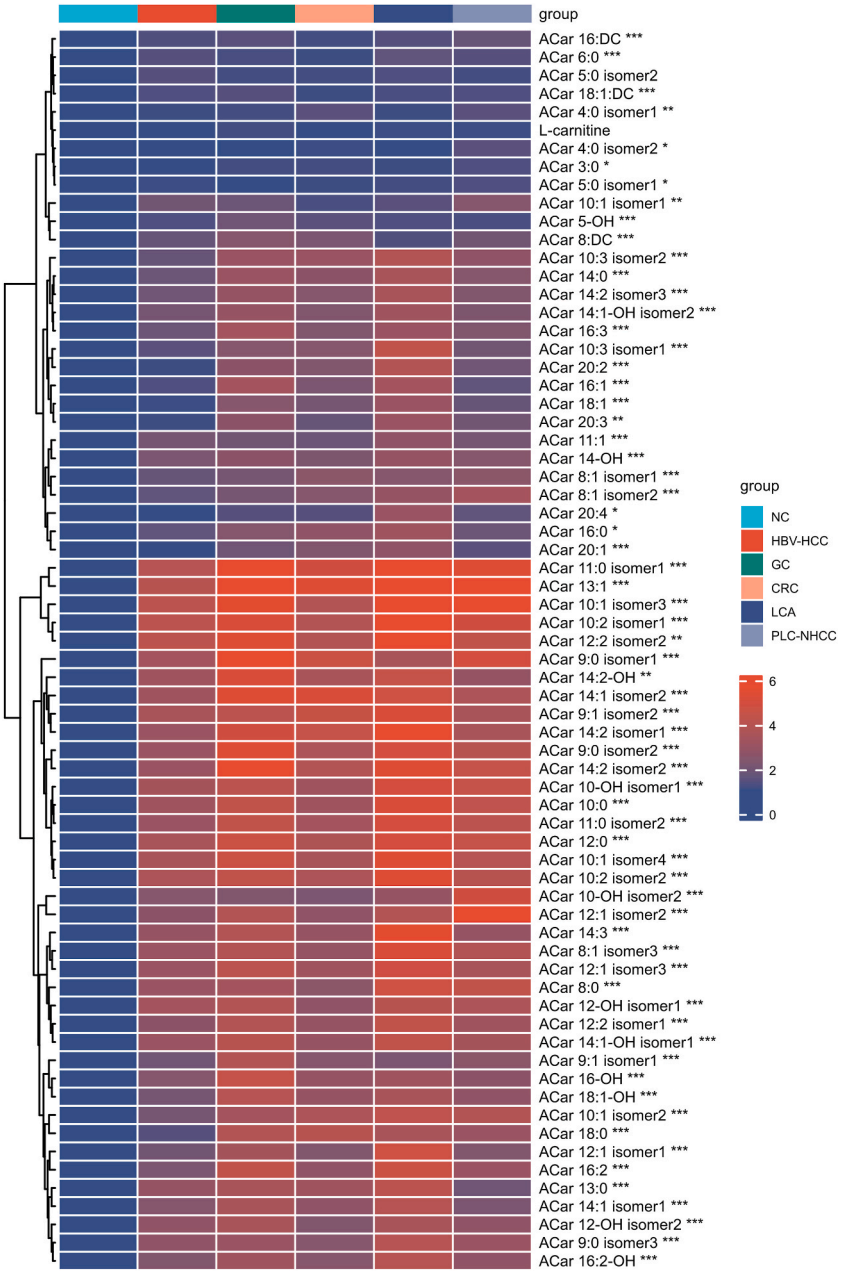

Fig. 2. Heat map of L-carnitine and 67 acylcarnitines in serum samples obtained from normal controls and patients with six types of solid tumors. Each row shows data for a specific acylcarnitine, and each column shows data for the normal controls and patients with solid tumors. The colors from blue to red showed fold changes (solid tumor vs. normal control groups). $^{*}P < 0.05$, $^{**}P < 0.01$, $^{***}P < 0.001$ determined by the Kruskal–Wallis test.

The AUC values of 16 ACars (C8–C14) for the diagnosis of six solid tumors were all >0.90, with those of ACar 10:2 isomer2 and 12:2 isomer2 being >0.95 (Table 5, Fig. 5). Therefore, 16 ACars (C8–C14) identified in this study have the potential to be used as serum biomarkers for the diagnosis of six types of solid tumors.

Three types of carnitine acyltransferases mediate the transfer of acyl groups to carnitine, forming short-, medium-, and long-chain ACars, respectively. Short-chain ACars (C2–C5) are thought to be the most abundant ACars in the body. Specifically, carnitine acetyltransferase is primarily responsible for the synthesis of both short-chain (≤C5) and branched ACars. Moreover, most short-chain ACars are the products of amino acid oxidation [36]. Reportedly, mitochondria can metabolize several straight-chain fatty acids, such as palmitic acid and oleic acid. However, those that cannot be metabolized by mitochondria are metabolized by peroxisome, including very long-chain fatty acids, dicarboxylic acids, bile acids, and branched fatty acids [37]. Another enzyme, carnitine

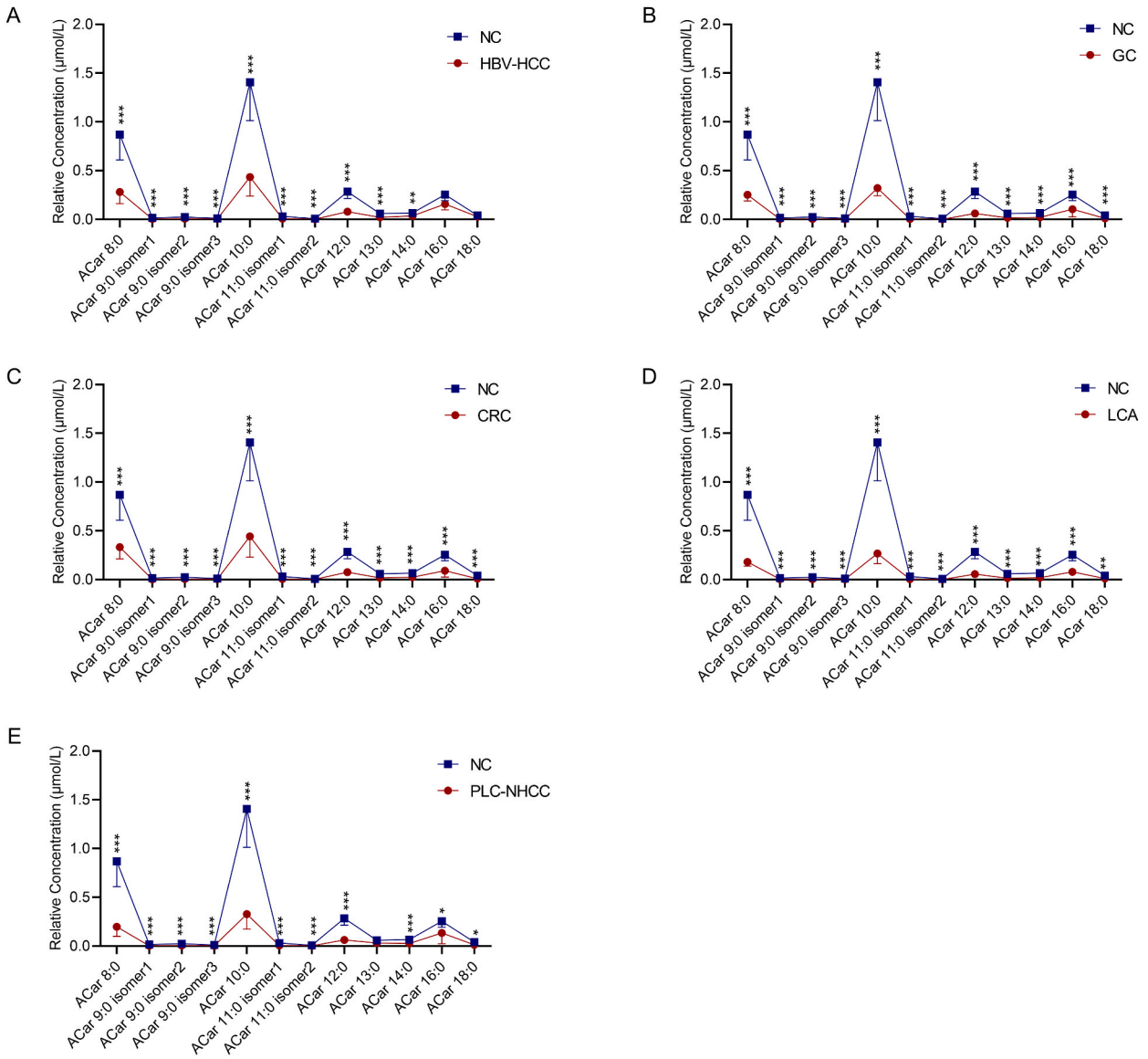

Fig. 3. Changes in medium- and long-chain, saturated acylcarnitines in various solid tumors. The relative concentrations of acylcarnitines of varying chain lengths were compared in the NC group with those in the HBV-HCC (A), GC (B), CRC (C), LCA (D), and PLC-NHCC groups (E). $^{*}P < 0.05$, $^{**}P < 0.01$, $^{***}P < 0.001$ determined by the Kruskal–Wallis test.

octanoyltransferase (COT) is primarily responsible for the synthesis of medium-chain (C6–C12) and branched ACars in peroxisomes. Another important source of medium-chain ACars is following peroxisome-mediated metabolism of long, very-long, and branched fatty acids. After peroxisome-mediated metabolism, medium-chain ACars are usually transported into the mitochondria for final mitochondrial metabolism [38]. With regard to long-chain ACars (>C12), these compounds are the product of the esterification of L-carnitine with long-chain fatty acids obtained from the diet. Most long-chain ACars are accumulated during incomplete FAO. And the expression of CPT1 and the availability of substrates are essential for long-chain ACar synthesis [34]. Therefore, short-, medium- and long-chain ACars are synthesized by different carnitine acyltransferase and via several metabolic pathways. The most significantly altered serum ACars (C8–C16) in six solid tumor types may be closely associated with peroxisomal and mitochondrial metabolic pathways. Peroxisomes may be primarily responsible for synthesizing these ACars, whereas mitochondria may be responsible for metabolizing the ACars. However, the mechanism underlying the selective ACar uptake remains to be elucidated.

The Warburg effect is a crucial aspect of tumor cell metabolism, in which most cancer cells obtain their energy primarily via glycolysis [39]. However, in recent years, increasing consideration is being given to the reprogramming of tumor lipid metabolism [40]. Although the reactivation of fatty acid synthesis has been identified as a part of metabolic reprogramming, the activation of FAO pathways is equally critical for the survival of several types of cancer cells [41]. Specifically, FAO may function as an extended aspect

Table 5
Sixteen acylcarnitines with an AUC of >0.90 for the diagnosis of the studied solid tumors.

No.	Metabolite	Isomer	(M + H)+	RT (min)	AUC NC vs HBV-HCC	NC vs GC	NC vs CRC	NC vs LCA	NC vs PLC-NHCC
1	ACar 11:0	isomer1	330.2639	9.86	0.973	0.983	0.966	0.987	0.904
2	ACar 8:1	isomer3	286.2013	6.94	0.960	0.975	0.913	0.963	0.967
3	ACar 9:1	isomer2	300.2168	7.52	0.914	0.981	0.949	0.922	0.916
4	ACar 10:1	isomer4	314.2324	8.92	0.990	1.000	0.945	0.991	0.978
5	ACar 12:1	isomer2	342.2641	10.42	0.950	0.983	0.910	0.968	0.967
6	ACar 12:1	isomer3	342.2641	10.57	0.958	0.991	0.930	0.977	0.978
7	ACar 13:1		356.2797	10.80	0.959	0.952	0.911	0.983	0.958
8	ACar 14:1	isomer2	370.2951	11.62	0.933	0.981	0.923	0.985	0.942
9	ACar 10:2	isomer1	312.2170	7.74	0.968	0.970	0.918	0.972	0.940
10	ACar 10:2[a]	isomer2[a]	312.2170	7.94	0.975	0.978	0.962	0.982	0.962
11	ACar 12:2	isomer1	340.2486	9.67	0.938	0.978	0.921	0.967	0.956
12	ACar 12:2[a]	isomer2[a]	340.2486	9.82	0.980	0.994	0.959	0.992	0.991
13	ACar 14:2	isomer2	368.2797	10.99	0.936	0.983	0.922	0.983	0.958
14	ACar 10-OH	isomer1	332.2433	7.51	0.959	0.983	0.912	0.960	0.976
15	ACar 14:1-OH	isomer1	386.2903	10.10	0.943	0.981	0.926	0.977	0.949
16	ACar 14:2-OH		384.2747	9.53	0.941	0.961	0.918	0.965	0.960

[a] Acylcarnitines with all AUC values > 0.95 for the diagnosis of the studied solid tumors. AUC: Area under the curve; RT: Retention time.; ACar: Acylcarnitine.

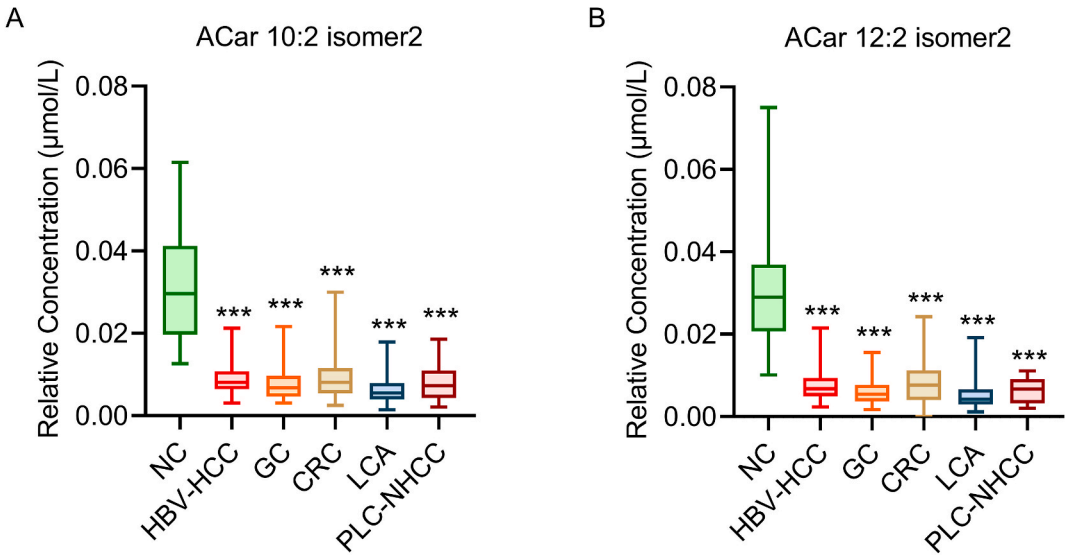

Fig. 4. Relative concentrations of ACar 10:2 isomer2 and 12:2 isomer2 in different solid tumors. Relative concentrations of serum ACar 10:2 isomer2 (A) and ACar 12:2 isomer2 (B) in different solid tumors. ***$P < 0.001$ when compared to the NC group.

of lipid metabolism by promoting energy production, eliminating potentially toxic lipids, and synthesizing metabolic intermediates for cell growth [42]. Particularly in cancer TME, FAO may play a crucial role. In addition, emerging studies have highlighted that cancer metabolism and behavior are regulated by the TME [19]. Cancer cells adapt to the harsh TME via metabolic reprogramming. Particularly, acidosis drives the metabolism of cancer cells towards FAO via changes in mitochondrial and histone acetylation [16]. In addition, multiple types of cancers have been demonstrated to rely on FAO for cell growth and survival under acidosis [43–46]. Reportedly, the activation of FAO pathways in tumor cells is mainly triggered by acidosis in the TME. As a result, FAO can be perceived as a metabolic pathway dependent on TME. Hypoxia is another important feature of solid tumors. Mammal cells have evolved key adaptive mechanisms to cope with hypoxia. Hypoxic cells adapt to hypoxia by modulating protein synthesis, metabolism, and nutrient uptake [14]>. Peroxisomes play an important role in lipid metabolism, with their function being highly dependent on molecular oxygen [11]>. Hif-2α promotes the selective autophagy of peroxisomes, resulting in their degradation [15]. The decrease in peroxisome abundance had an important effect on the lipid composition. Medium-chain ACars are the main products of very long-chain fatty acids and polyunsaturated fatty acids degraded by peroxisomes. Thus, the reduction of medium- and long-chain ACars in solid tumors may result from the combined effects of hypoxia and acidosis. Normal and cancer cells in regions of hypoxia and acidosis may have evolved mechanisms to adapt to the unfavorable TME. Hypoxia and acidosis are universal features of solid tumors. These results

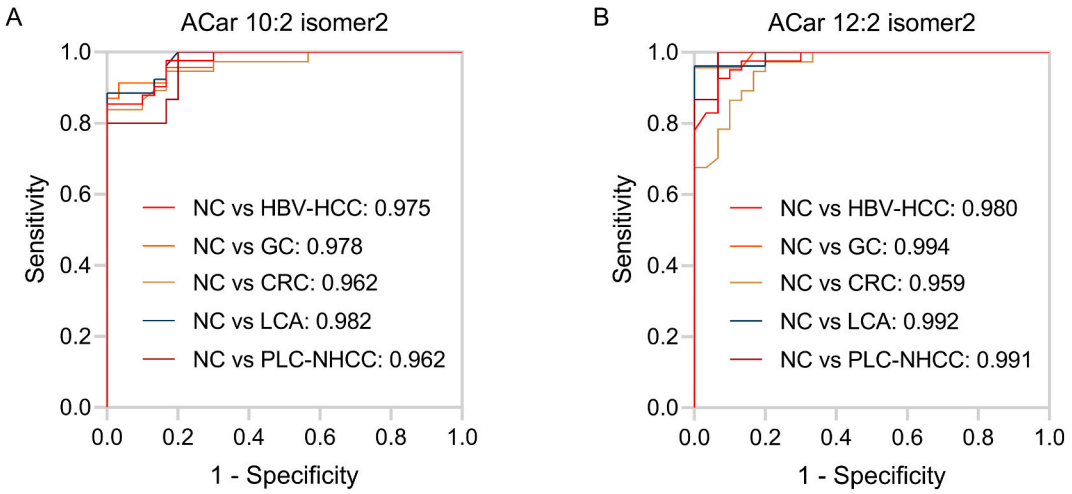

Fig. 5. ROC analysis revealed the diagnostic ability of ACar 10:2 isomer2 and ACar 12:2 isomer2. Diagnostic ability of ACar 10:2 isomer2 (A) and ACar 12:2 isomer2 (B) in various solid tumors. The corresponding areas under the curve are represented.

suggest that profiling ACars in human serum may play an important role in the detection of various solid tumors.

ACars are being increasingly recognized as important biomarkers for metabolic studies in various diseases, including inborn metabolic diseases, cardiovascular diseases, depression, metabolic disorders, diabetes, Alzheimer's disease, and certain types of cancer [34]. A study has reported the downregulation of medium-chain ACars and upregulation of long-chain ACars in HCC tissue compared with distal noncancerous tissues [23]. In addition, patients with HCC have been demonstrated to have higher levels of serum-saturated long-chain ACars and lower levels of short- and medium-chain ACars [47,48]. Particularly, obesity- and nonalcoholic steatohepatitis-related HCC is characterized by the downregulation of CPT2, which increases the accumulation of ACars, allowing HCC cells to avoid lipotoxicity and promote hepatocarcinogenesis [25]. In patients with CRC, cancer cells were found to accumulate long-chain ACars, unlike the paired normal tissues [29]. Moreover, the plasma levels of medium-chain ACars (ACar 8:0, 9:0, 10:0, and 11:0) were significantly lower in patients with esophageal squamous cell carcinoma than in the healthy control group [49]. Thus, the serum levels of medium-chain ACars are generally lower in patients with solid tumors than in healthy controls, whereas the opposite is true for long-chain ACars. Moreover, previous studies have reported metabolic dysregulation of ACar 11:0, 10:1, 12:1, and 14:1-OH in some cancers [23,26,49–51], with few studies reporting the utility of unsaturated ACars as diagnostic biomarkers. The present study identified 16 ACars (AUC >0.90) with diagnostic potential in six solid tumors (Table 5). In addition to the four previously reported ACars, we determined 12 unreported differential ACars as potential diagnostic biomarkers for solid tumors.

FAO enzymes are overexpressed in several malignant tumors [17]. Inhibiting the rate-limiting enzyme CPT1 in FAO has the potential to both delay and prolong tumor survival [13,52]. Furthermore, in HepG2 human hepatocytes, COT overexpression was found to decrease the levels of medium-chain fatty acids, indicating increased FAO [53]. As the six solid tumors assessed in the present study may share the similar metabolic pathway, simultaneous targeted inhibition of CPT and COT may be a more effective strategy for cancer treatment.

Owing to a lack of commercially available ACar standards, the present study used a relative quantitative method to analyze the serum ACars. Lacking information regarding tumor size, comorbidities, and the treatment of tumors or comorbidities is a weakness in the study. Meanwhile, we lack ACar profiling for non-tumor diseases, which could aid in understanding tumor etiology and progression. Furthermore, the steady state, uptake, and metabolism of the acylcarnitine profile in tumors were not measured, which is the limitation of the study. Therefore, the mechanism underlying ACar metabolism in solid tumor cells is currently unclear. Future research aims to address the limitations noted above.

In conclusion, we comprehensively investigated 69 ACars in six solid tumor types and NCs using a targeted analysis method employing UHPLC-MS/MS. A significant alteration was noted in ACar levels that was linked to chain lengths and saturation. In addition, the marked decrease in medium- and long-chain ACars (C8–C18) in the six solid tumors suggests that these metabolites may share the similar FAO metabolic pathways. Sixteen ACars (C8–C14), especially ACar 10:2 isomer2 and 12:2 isomer2, were identified as potential biomarkers for the diagnosis of six solid tumors. The characteristic alterations observed in medium- and long-chain ACars could serve as valuable references for the diagnosis of solid tumors and potential targets for cancer treatment.

Funding statement

Yuandong Li was supported by the National Natural Science Foundation of China [grant numbers 81860527].

Ethics declarations

This study was reviewed and approved by [the Medical Ethics Committee of the Guangxi Medical University Cancer Hospital], with the approval number: [LW2022127].

All participants/patients (or their proxies/legal guardians) provided informed consent to participate in the study.

Data availability statement

Data included in article/supplementary material/referenced in article.

CRediT authorship contribution statement

Longjunyu Wu: Writing – original draft, Formal analysis, Data curation. **Chunhua Ye:** Writing – original draft, Formal analysis, Data curation. **Qingchun Yao:** Formal analysis, Data curation. **Qianqian Li:** Formal analysis. **Chunyan Zhang:** Writing – review & editing, Conceptualization. **Yuandong Li:** Writing – review & editing, Methodology, Funding acquisition, Conceptualization.

Declaration of competing interest

The authors declare that they have no known competing financial interests or personal relationships that could have appeared to influence the work reported in this paper.

Appendix A. Supplementary data

Supplementary data to this article can be found online at https://doi.org/10.1016/j.heliyon.2023.e23867.

References

[1] H. Sung, J. Ferlay, R.L. Siegel, M. Laversanne, I. Soerjomataram, A. Jemal, F. Bray, Global cancer statistics 2020: GLOBOCAN estimates of incidence and mortality worldwide for 36 cancers in 185 countries, CA A Cancer J. Clin. 71 (2021) 209–249, https://doi.org/10.3322/caac.21660.
[2] A. Mattox, C. Bettegowda, S. Zhou, N. Papadopoulos, K. Kinzler, B. Vogelstein, Applications of liquid biopsies for cancer, Sci. Transl. Med. 11 (2019), https://doi.org/10.1126/scitranslmed.aay1984.
[3] D.W. Cescon, S.V. Bratman, S.M. Chan, L.L. Siu, Circulating tumor DNA and liquid biopsy in oncology, Nat. Can. (Ott.) 1 (2020) 276–290, https://doi.org/10.1038/s43018-020-0043-5.
[4] M.F. Berger, E.R. Mardis, The emerging clinical relevance of genomics in cancer medicine, Nat. Rev. Clin. Oncol. 15 (2018) 353–365, https://doi.org/10.1038/s41571-018-0002-6.
[5] L.A. Diaz Jr., A. Bardelli, Liquid biopsies: genotyping circulating tumor DNA, J. Clin. Oncol. 32 (2014) 579–586, https://doi.org/10.1200/JCO.2012.45.2011.
[6] P.S. Ward, C.B. Thompson, Metabolic reprogramming: a cancer hallmark even warburg did not anticipate, Cancer Cell 21 (2012) 297–308, https://doi.org/10.1016/j.ccr.2012.02.014.
[7] O. Warburg, On the origin of cancer cells, Science (New York, NY) 123 (1956) 309–314, https://doi.org/10.1126/science.123.3191.309.
[8] M.V. Liberti, J.W. Locasale, The warburg effect: how does it benefit cancer cells? Trends Biochem. Sci. 41 (2016) 211–218, https://doi.org/10.1016/j.tibs.2015.12.001.
[9] C.M. Metallo, P.A. Gameiro, E.L. Bell, K.R. Mattaini, J. Yang, K. Hiller, C.M. Jewell, Z.R. Johnson, D.J. Irvine, L. Guarente, J.K. Kelleher, M.G. Vander Heiden, O. Iliopoulos, G. Stephanopoulos, Reductive glutamine metabolism by IDH1 mediates lipogenesis under hypoxia, Nature 481 (2011) 380–384, https://doi.org/10.1038/nature10602.
[10] B. Reinfeld, M. Madden, M. Wolf, A. Chytil, J. Bader, A. Patterson, A. Sugiura, A. Cohen, A. Ali, B. Do, A. Muir, C. Lewis, R. Hongo, K. Young, R. Brown, V. Todd, T. Huffstater, A. Abraham, R. O'neil, M. Wilson, F. Xin, M. Tantawy, W. Merryman, R. Johnson, C. Williams, E. Mason, F. Mason, K. Beckermann, M. Vander Heiden, H. Manning, J. Rathmell, W. Rathmell, Cell-programmed nutrient partitioning in the tumour microenvironment, Nature 593 (2021) 282–288, https://doi.org/10.1038/s41586-021-03442-1.
[11] M.S. Nakazawa, B. Keith, M.C. Simon, Oxygen availability and metabolic adaptations, Nat. Rev. Cancer 16 (2016) 663–673, https://doi.org/10.1038/nrc.2016.84.
[12] M.S. Padanad, G. Konstantinidou, N. Venkateswaran, M. Melegari, S. Rindhe, M. Mitsche, C. Yang, K. Batten, K.E. Huffman, J. Liu, X. Tang, J. Rodriguez-Canales, N. Kalhor, J.W. Shay, J.D. Minna, J. Mcdonald, Ii Wistuba, R.J. Deberardinis, P.P. Scaglioni, Fatty acid oxidation mediated by acyl-CoA synthetase long chain 3 is required for mutant KRAS lung tumorigenesis, Cell Rep. 16 (2016) 1614–1628, https://doi.org/10.1016/j.celrep.2016.07.009.
[13] R. Camarda, A.Y. Zhou, R.A. Kohnz, S. Balakrishnan, C. Mahieu, B. Anderton, H. Eyob, S. Kajimura, A. Tward, G. Krings, D.K. Nomura, A. Goga, Inhibition of fatty acid oxidation as a therapy for MYC-overexpressing triple-negative breast cancer, Nat. Med. 22 (2016) 427–432, https://doi.org/10.1038/nm.4055.
[14] P. Lee, N.S. Chandel, M.C. Simon, Cellular adaptation to hypoxia through hypoxia inducible factors and beyond, Nat. Rev. Mol. Cell Biol. 21 (2020) 268–283, https://doi.org/10.1038/s41580-020-0227-y.
[15] K.M. Walter, M.J. Schonenberger, M. Trotzmuller, M. Horn, H.P. Elsasser, A.B. Moser, M.S. Lucas, T. Schwarz, P.A. Gerber, P.L. Faust, H. Moch, H.C. Kofeler, W. Krek, W.J. Kovacs, Hif-2alpha promotes degradation of mammalian peroxisomes by selective autophagy, Cell Metabol. 20 (2014) 882–897, https://doi.org/10.1016/j.cmet.2014.09.017.
[16] C. Corbet, A. Pinto, R. Martherus, J.P. Santiago De Jesus, F. Polet, O. Feron, Acidosis drives the reprogramming of fatty acid metabolism in cancer cells through changes in mitochondrial and histone acetylation, Cell Metabol. 24 (2016) 311–323, https://doi.org/10.1016/j.cmet.2016.07.003.
[17] Y. Ma, S.M. Temkin, A.M. Hawkridge, C. Guo, W. Wang, X.Y. Wang, X. Fang, Fatty acid oxidation: an emerging facet of metabolic transformation in cancer, Cancer Lett. 435 (2018) 92–100, https://doi.org/10.1016/j.canlet.2018.08.006.
[18] P. Acebo, D. Giner, P. Calvo, A. Blanco-Rivero, A.D. Ortega, P.L. Fernandez, G. Roncador, E. Fernandez-Malave, M. Chamorro, J.M. Cuezva, Cancer abolishes the tissue type-specific differences in the phenotype of energetic metabolism, Transl Oncol 2 (2009) 138–145, https://doi.org/10.1593/tlo.09106.
[19] I. Elia, M.C. Haigis, Metabolites and the tumour microenvironment: from cellular mechanisms to systemic metabolism, Nat. Metab. 3 (2021) 21–32, https://doi.org/10.1038/s42255-020-00317-z.

[20] S. Li, D. Gao, Y. Jiang, Function, detection and alteration of acylcarnitine metabolism in hepatocellular carcinoma, Metabolites 9 (2019), https://doi.org/10.3390/metabo9020036.

[21] T.N. Tarasenko, K. Cusmano-Ozog, P.J. Mcguire, Tissue acylcarnitine status in a mouse model of mitochondrial beta-oxidation deficiency during metabolic decompensation due to influenza virus infection, Mol. Genet. Metabol. 125 (2018) 144–152, https://doi.org/10.1016/j.ymgme.2018.06.012.

[22] Y. Wang, Y. Chen, L. Guan, H. Zhang, Y. Huang, C.H. Johnson, Z. Wu, F.J. Gonzalez, A. Yu, P. Huang, Y. Wang, S. Yang, P. Chen, X. Fan, M. Huang, H. Bi, Carnitine palmitoyltransferase 1C regulates cancer cell senescence through mitochondria-associated metabolic reprograming, Cell Death Differ. 25 (2018) 735–748, https://doi.org/10.1038/s41418-017-0013-3.

[23] Y. Lu, N. Li, L. Gao, Y.J. Xu, C. Huang, K. Yu, Q. Ling, Q. Cheng, S. Chen, M. Zhu, J. Fang, M. Chen, C.N. Ong, Acetylcarnitine is a candidate diagnostic and prognostic biomarker of hepatocellular carcinoma, Cancer Res. 76 (2016) 2912–2920, https://doi.org/10.1158/0008-5472.CAN-15-3199.

[24] D.J. Kim, E.J. Cho, K.S. Yu, I.J. Jang, J.H. Yoon, T. Park, J.Y. Cho, Comprehensive metabolomic search for biomarkers to differentiate early stage hepatocellular carcinoma from cirrhosis, Cancers 11 (2019), https://doi.org/10.3390/cancers11101497. Basel.

[25] N. Fujiwara, H. Nakagawa, K. Enooku, Y. Kudo, Y. Hayata, T. Nakatsuka, Y. Tanaka, R. Tateishi, Y. Hikiba, K. Misumi, M. Tanaka, A. Hayashi, J. Shibahara, M. Fukayama, J. Arita, K. Hasegawa, H. Hirschfield, Y. Hoshida, Y. Hirata, M. Otsuka, K. Tateishi, K. Koike, CPT2 downregulation adapts HCC to lipid-rich environment and promotes carcinogenesis via acylcarnitine accumulation in obesity, Gut 67 (2018) 1493–1504, https://doi.org/10.1136/gutjnl-2017-315193.

[26] F. Zhao, R. An, L. Wang, J. Shan, X. Wang, Specific gut microbiome and serum metabolome changes in lung cancer patients, Front. Cell. Infect. Microbiol. 11 (2021), 725284, https://doi.org/10.3389/fcimb.2021.725284.

[27] A. Klupczynska, P. Derezinski, T.J. Garrett, V.Y. Rubio, W. Dyszkiewicz, M. Kasprzyk, Z.J. Kokot, Study of early stage non-small-cell lung cancer using Orbitrap-based global serum metabolomics, J. Cancer Res. Clin. Oncol. 143 (2017) 649–659, https://doi.org/10.1007/s00432-017-2347-0.

[28] Y. Jing, X. Wu, P. Gao, Z. Fang, J. Wu, Q. Wang, C. Li, Z. Zhu, Y. Cao, Rapid differentiating colorectal cancer and colorectal polyp using dried blood spot mass spectrometry metabolomic approach, IUBMB Life 69 (2017) 347–354, https://doi.org/10.1002/iub.1617.

[29] Y. Shen, M. Sun, J. Zhu, M. Wei, H. Li, P. Zhao, J. Wang, R. Li, L. Tian, Y. Tao, P. Shen, J. Zhang, Tissue metabolic profiling reveals major metabolic alteration in colorectal cancer, Mol Omics 17 (2021) 464–471, https://doi.org/10.1039/d1mo00022e.

[30] G. Corona, R. Cannizzaro, G. Miolo, L. Caggiari, M. De Zorzi, O. Repetto, A. Steffan, V. De Re, Use of metabolomics as a complementary omic approach to implement risk criteria for first-degree relatives of gastric cancer patients, Int. J. Mol. Sci. 19 (2018), https://doi.org/10.3390/ijms19030750.

[31] P.E. Minkler, M.S. Stoll, S.T. Ingalls, J. Kerner, C.L. Hoppel, Validated method for the quantification of free and total carnitine, butyrobetaine, and acylcarnitines in biological samples, Anal. Chem. 87 (2015) 8994–9001, https://doi.org/10.1021/acs.analchem.5b02198.

[32] D. Yu, L. Zhou, Q. Xuan, L. Wang, X. Zhao, X. Lu, G. Xu, Strategy for comprehensive identification of acylcarnitines based on liquid chromatography-high-resolution mass spectrometry, Anal. Chem. 90 (2018) 5712–5718, https://doi.org/10.1021/acs.analchem.7b05471.

[33] C. Indiveri, V. Iacobazzi, A. Tonazzi, N. Giangregorio, V. Infantino, P. Convertini, L. Console, F. Palmieri, The mitochondrial carnitine/acylcarnitine carrier: function, structure and physiopathology, Mol. Aspect. Med. 32 (2011) 223–233, https://doi.org/10.1016/j.mam.2011.10.008.

[34] M. Dambrova, M. Makrecka-Kuka, J. Kuka, R. Vilskersts, D. Nordberg, M. Attwood, S. Smesny, Z. Sen, A. Guo, E. Oler, S. Tian, J. Zheng, D. Wishart, E. Liepinsh, H. Schiöth, Acylcarnitines: nomenclature, biomarkers, therapeutic potential, drug targets, and clinical trials, Pharmacol. Rev. 74 (2022) 506–551, https://doi.org/10.1124/pharmrev.121.000408.

[35] A.A. Papamandjaris, D.E. Macdougall, P.J. Jones, Medium chain fatty acid metabolism and energy expenditure: obesity treatment implications, Life Sci. 62 (1998) 1203–1215, https://doi.org/10.1016/s0024-3205(97)01143-0.

[36] P. Giesbertz, J. Ecker, A. Haag, B. Spanier, H. Daniel, An LC-MS/MS method to quantify acylcarnitine species including isomeric and odd-numbered forms in plasma and tissues, J. Lipid Res. 56 (2015) 2029–2039, https://doi.org/10.1194/jlr.D061721.

[37] S.M. Houten, R.J.A. Wanders, P. Ranea-Robles, Metabolic interactions between peroxisomes and mitochondria with a special focus on acylcarnitine metabolism, Biochim. Biophys. Acta, Mol. Basis Dis. 1866 (2020), 165720, https://doi.org/10.1016/j.bbadis.2020.165720.

[38] S. Violante, N. Achetib, C.W.T. Van Roermund, J. Hagen, T. Dodatko, F.M. Vaz, H.R. Waterham, H. Chen, M. Baes, C. Yu, C.A. Argmann, S.M. Houten, Peroxisomes can oxidize medium- and long-chain fatty acids through a pathway involving ABCD3 and HSD17B4, Faseb. J. 33 (2019) 4355–4364, https://doi.org/10.1096/fj.201801498R.

[39] M.G. Vander Heiden, L.C. Cantley, C.B. Thompson, Understanding the Warburg effect: the metabolic requirements of cell proliferation, Science 324 (2009) 1029–1033, https://doi.org/10.1126/science.1160809.

[40] M. Sangineto, R. Villani, F. Cavallone, A. Romano, D. Loizzi, G. Serviddio, Lipid metabolism in development and progression of hepatocellular carcinoma, Cancers 12 (2020), https://doi.org/10.3390/cancers12061419.

[41] M.T. Snaebjornsson, S. Janaki-Raman, A. Schulze, Greasing the wheels of the cancer machine: the role of lipid metabolism in cancer, Cell Metabol. 31 (2020) 62–76, https://doi.org/10.1016/j.cmet.2019.11.010.

[42] A. Carracedo, L.C. Cantley, P.P. Pandolfi, Cancer metabolism: fatty acid oxidation in the limelight, Nat. Rev. Cancer 13 (2013) 227–232, https://doi.org/10.1038/nrc3483.

[43] N.N. Pavlova, C.B. Thompson, The emerging hallmarks of cancer metabolism, Cell Metabol. 23 (2016) 27–47, https://doi.org/10.1016/j.cmet.2015.12.006.

[44] P. Caro, A. Kishan, E. Norberg, I. Stanley, B. Chapuy, S. Ficarro, K. Polak, D. Tondera, J. Gounarides, H. Yin, F. Zhou, M. Green, L. Chen, S. Monti, J. Marto, M. Shipp, N. Danial, Metabolic signatures uncover distinct targets in molecular subsets of diffuse large B cell lymphoma, Cancer Cell 22 (2012) 547–560, https://doi.org/10.1016/j.ccr.2012.08.014.

[45] S. Zha, S. Ferdinandusse, J. Hicks, S. Denis, T. Dunn, R. Wanders, J. Luo, A. De Marzo, W. Isaacs, Peroxisomal branched chain fatty acid beta-oxidation pathway is upregulated in prostate cancer, Prostate 63 (2005) 316–323, https://doi.org/10.1002/pros.20177.

[46] I. Samudio, R. Harmancey, M. Fiegl, H. Kantarjian, M. Konopleva, B. Korchin, K. Kaluarachchi, W. Bornmann, S. Duvvuri, H. Taegtmeyer, M. Andreeff, Pharmacologic inhibition of fatty acid oxidation sensitizes human leukemia cells to apoptosis induction, J. Clin. Invest. 120 (2010) 142–156, https://doi.org/10.1172/JCI38942.

[47] S. Chen, H. Kong, X. Lu, Y. Li, P. Yin, Z. Zeng, G. Xu, Pseudotargeted metabolomics method and its application in serum biomarker discovery for hepatocellular carcinoma based on ultra high-performance liquid chromatography/triple quadrupole mass spectrometry, Anal. Chem. 85 (2013) 8326–8333, https://doi.org/10.1021/ac4016787.

[48] X. Lu, X. Zhang, Y. Zhang, K. Zhang, C. Zhan, X. Shi, Y. Li, J. Zhao, Y. Bai, Y. Wang, H. Nie, Y. Li, Metabolic profiling analysis upon acylcarnitines in tissues of hepatocellular carcinoma revealed the inhibited carnitine shuttle system caused by the downregulated carnitine palmitoyltransferase 2, Mol. Carcinog. 58 (2019) 749–759, https://doi.org/10.1002/mc.22967.

[49] J. Xu, Y. Chen, R. Zhang, Y. Song, J. Cao, N. Bi, J. Wang, J. He, J. Bai, L. Dong, L. Wang, Q. Zhan, Z. Abliz, Global and targeted metabolomics of esophageal squamous cell carcinoma discovers potential diagnostic and therapeutic biomarkers, Mol. Cell. Proteomics : MCP 12 (2013) 1306–1318, https://doi.org/10.1074/mcp.M112.022830.

[50] C. Ruiying, L. Zeyun, Y. Yongliang, Z. Zijia, Z. Ji, T. Xin, Z. Xiaojian, A comprehensive analysis of metabolomics and transcriptomics in non-small cell lung cancer, PLoS One 15 (2020), e0232272, https://doi.org/10.1371/journal.pone.0232272.

[51] J. Niziol, V. Bonifay, K. Ossolinski, T. Ossolinski, A. Ossolinska, J. Sunner, I. Beech, A. Arendowski, T. Ruman, Metabolomic study of human tissue and urine in clear cell renal carcinoma by LC-HRMS and PLS-DA, Anal. Bioanal. Chem. 410 (2018) 3859–3869, https://doi.org/10.1007/s00216-018-1059-x.

[52] H. Lin, S. Patel, V.S. Affleck, I. Wilson, D.M. Turnbull, A.R. Joshi, R. Maxwell, E.A. Stoll, Fatty acid oxidation is required for the respiration and proliferation of malignant glioma cells, Neuro Oncol. 19 (2017) 43–54, https://doi.org/10.1093/neuonc/now128.

[53] F. Le Borgne, A. Ben Mohamed, M. Logerot, E. Garnier, J. Demarquoy, Changes in carnitine octanoyltransferase activity induce alteration in fatty acid metabolism, Biochem. Biophys. Res. Commun. 409 (2011) 699–704, https://doi.org/10.1016/j.bbrc.2011.05.068.